ARTICLES

The Interplay of Hydrophobic and Electrostatic Effects in the Surfactant-Induced Aggregation/Deaggregation of Chlorin p_6

Padmaja P. Mishra, Jaya Bhatnagar, and Anindya Datta*

Department of Chemistry, Indian Institute of Technology, Bombay, Powai, Mumbai 400 076, India

Received: May 22, 2005; In Final Form: October 27, 2005

The aggregation/deaggregation of chlorin p_6 with the surfactants CTAB, SDS, and TX 100 have been studied by using absorption, fluorescence, and light scattering techniques. The ionic surfactants are found to cause aggregation of fluorophore at submicellar concentrations. The aggregates dissolve at higher surfactant concentrations to yield micellized monomers. This is rationalized by the interplay of electrostatic and hydrophobic effects. A prominent pH effect is observed in the ionic surfactant induced aggregation process as the charge on the fluorophore is controlled by the pH of the medium. Interestingly, the neutral TX-100 also induces aggregation of chlorin p_6 at low concentrations, indicating that hydrophobic effects by themselves can cause aggregation unless there is a hindrance by repulsive electrostatic effects.

Introduction

The photochemical and photophysical study of complex systems is important in understanding the function associated with them.[1] Such systems are ubiquitous in nature, from nonliving atoms and molecules, to living cells and organisms. Molecular aggregates are examples of such complex systems formed by self-assembly, involving noncovalent intermolecular forces.[2] These aggregates have generated considerable interest for a long time because of their unique spectroscopic and electronic properties arising from the excitonic interactions.[2−4] Studies of such aggregates can serve to provide an understanding of the changing properties of matter with size and the onset of new optical phenomena and can lead the development of new materials.[5−7]

Porphyrins are a class of compounds which are known to form aggregates of different kinds.[8,9] This is an important factor that affects their activity in membranes. Depending upon the molecular arrangement, these aggregates are classified as J, H, or random aggregates.[3,8−12] The process of aggregation can be influenced by different physicochemical properties of the membrane,[13] the bulk pH of aqueous medium,[14,15] and the hydrophobicity of the porphyrin, which in turn is affected by the presence or absence of charged or polar groups on the frame of the macrocycle.[16,17] This is important in understanding the activity of porphyrins in photosynthetic systems as well as in Photodynamic therapy (PDT), which is based on the selective localization of the photosensitizer and the subsequent irradiation to generate cytotoxic species.[18−22] The mechanisms of biological effects of porphyrins and metalloporphyrins may involve their penetration through membranes and binding to intracellular organelles.[23] Therefore, incorporation of porphyrins in biomimetic membranes have attracted a lot of attention.[24,25] This is the impetus for us to undertake a systematic investigation of chlorin p_6 in micelles.

SCHEME 1: Structures of p_6

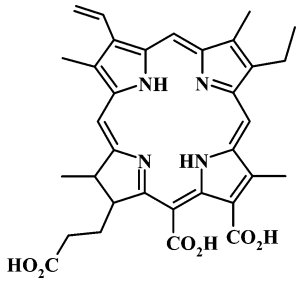

Earlier, we have reported the pH-induced aggregation of chlorin p_6 (Scheme 1).[15] The fluorophore exists as an anion at pH 7 due to the presence of three carboxylic acids groups, all of which are expected to be ionized at this pH. Since no change is observed in the absorption spectrum above this pH, it can be concluded that no further ionization takes place above this pH. Fluorescence quantum yield is also constant over this range. On decreasing the pH to 3, the Soret band in the absorption spectrum undergoes a red shift whereas the Q-band undergoes a blue shift with the development of a new aggregate band at 675 nm. This is explained by the protonation of one or more carboxylic acid groups and nitrogen atoms, which causes an increase in hydrophobicity and leads to aggregation of the fluorophore, which is nonfluorescent in nature. The aggregates dissociate at pH <3 due to further protonation of the three anionic carboxylate groups and the two ring nitrogen atoms,[15] similar to the earlier observations.[3−4,10−12,26] More recently, we have reported a preliminary fluorescence monitoring of the pH dependence of formation of chlorin p_6-surfactant aggregates, which have been found to form with the cationic CTAB at pH 7 and 5 and with the anionic SDS at pH 3.[27] We have also studied the electron transfer of chlorin p_6 with methyl viologen

* To whom correspondence should be addressed. Phone: +91-22-2576-7149. Fax: +91-22-2572-3480. E-mail: anindya@chem.iitb.ac.in.

10.1021/jp052682o CCC: $30.25
Published on Web 12/06/2005

in the presence of surfactants.[28] An effect of pH on the cellular uptake as well as liposome binding of chlorin p_6 have been reported very recently.[19,20] It has been noted that the pH effect is observed only for certain kinds of cell lines whereas for others, the uptake is determined by diffusional processes and shows no effect of pH. In the present work we have reported the detailed spectroscopic and light scattering studies on the influence of pH on the aggregation/deaggregation of chlorin p_6 by surfactants with positive, neutral, and negative headgroups. The results are interpreted in the light of interplay of hydrophobic and electrostatic effects.

Experimental Section

Materials. Chlorin p_6 has been prepared from dry spinach leaves following the procedure of Hoober et al.[29] The purity is tested by TLC, elemental analysis, superimposability of the absorption, and fluorescence excitation spectra. The concentration of fluorophore used is 7 μM. All the experiments have been carried out with this concentration. All chemicals used in the preparation of the buffers are from E-Merck, Mumbai, India. The AR grade surfactants cetyl trimethylammonium bromide (CTAB) and sodium dodecyl sulfate (SDS)were obtained from Aldrich chemicals US and used as such.

Absorbance, Fluorescence, and Light-Scattering Measurements. The steady-state UV/vis spectra have been measured on a JASCO V570 spectrophotometer. The fluorescence and resonance light scattering spectra have been recorded on a Perkin-Elmer LS55 fluorimeter. $\lambda_{ex} = 400$ nm has been used for measuring the fluorescence spectra. All the fluorescence spectra are corrected for the changes in absorbance. Fluorescence quantum yields (ϕ_f) are calculated by using Tetraphenyl porphyrin (TPP) as the standard ($\phi_f = 0.11$).[30] Resonance Light scattering (RLS) spectra have been recorded in the synchronous scan mode with zero offset in the range of 305 to 600 nm. The spectra are baseline corrected.[31−33]

Determination of Association Constant (K_b) with Surfactants. Three wavelengths, where prominent changes occur upon addition of surfactant, are used to calculate the constant of association. The data are fit to the following equation in order to obtain the association constant K_b[16,33]

$$A = A_f^0 + \frac{(A_b^0 - A_f^0)}{\frac{1}{K_b([S]_0 - \mathrm{cmc})^N} + 1} \quad (1)$$

where A = measured absorbance, A_f^0 = absorbance of the compound in the absence of surfactant, A_b^0 = absorbance of the surfactant-bound compound, $[S]_0$ = surfactant concentration, cmc = critical micellar concentration, and N = number of micelles/number of molecules of the compound.

Time-Resolved Emission Spectroscopy. For picosecond lifetime measurement, the IBH Fluorocube picosecond time correlated single photon counting (TCSPC) setup was used. The excitation light source used is a 406 nm diode laser. All the measurements are performed at a resolution of 7 ps/channel with the emission polarizer at magic angle (57.4°).

Dynamic Light-Scattering Studies. The dynamic light-scattering (DLS) measurements have been performed with a BI-MAS multiangle sizing Zeeta Plus instrument that uses a 15 mW continuous wave solid state laser of 660 nm as the light source. Intensity of the scattered light from the solution is measured in the perpendicular direction by an Avalanche Photodiode (APD). The DLS measurements of the aggregation have been performed by using the standard 1 cm quartz cuvette, which allows a sufficiently large volume for proper mixing of the components. All the solutions are prepared in Millipore water and further, to avoid the presence of any dust particles, the sample solutions are centrifuged with 10 000 rpm for 30 min.

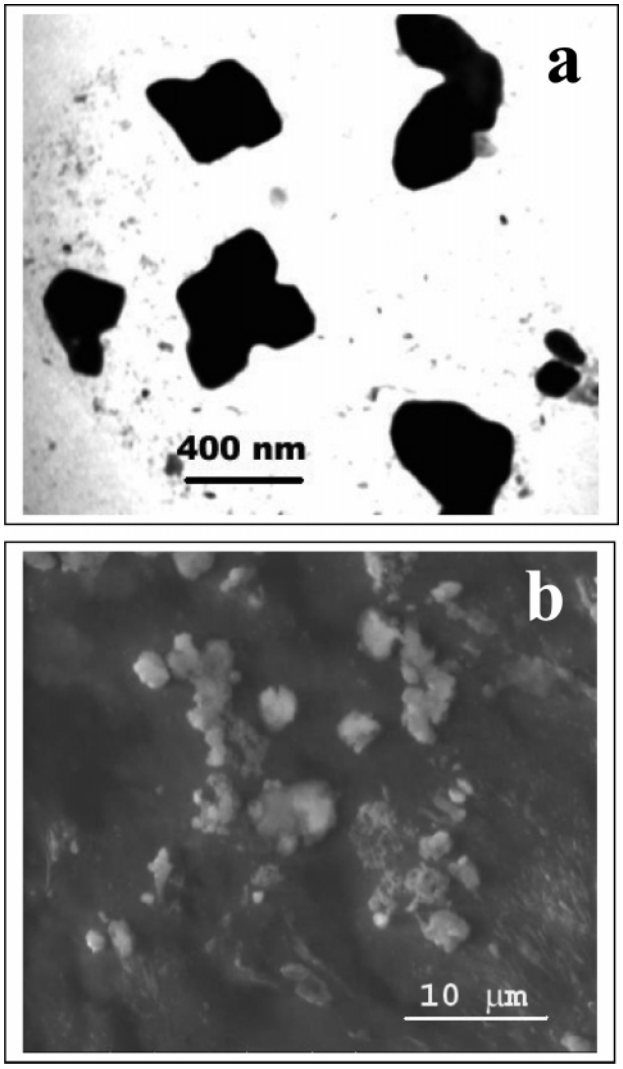

Figure 1. (a) Cryo-TEM and (b) SEM micrographs of chlorin p_6 at pH 3 buffer.

TEM and SEM Imaging. The aggregation morphology is monitored by Scanning electron microscopy (SEM) and Transmission electron microscopy (TEM) techniques by using a FET Quanta-200 instrument at low vacuum (0.98 Torr) and a cryo based TEM model TECNAI 20-G instrument, respectively. For SEM imaging, a droplet (~1 μL) of the sample is kept on a stainless steel stub and the imaging analyses have been done at low vacuum (0.98 Torr). For the TEM imaging, a drop of the sample (~1 μL) is placed on the sample holder and plunged into liquid nitrogen at high speed for fast cooling to avoid further recombination of the aggregates to form larger aggregates.

Results and Discussions

Absorption Spectra. As described in the earlier section, chlorin p_6 exists as monomers at pH 7 and as aggregated forms at pH 5 and 3. Figure 1 shows the TEM and SEM images of these aggregates at pH 3. The diameters of these aggregates obtained from the TEM image vary from 400 to 700 nm. Rather large aggregates of diameter 450 nm−2.5 μm are observed in SEM, possibly due to the further aggregation of the chlorin p_6

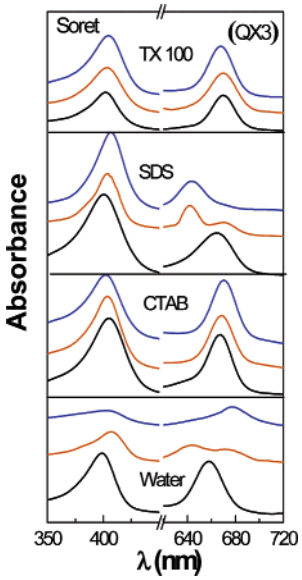

Figure 2. Principal absorption peaks of chlorin p_6 in aqueous buffers of pH 7 (black), 5 (orange), and 3 (blue) in the absence of surfactant and in the presence of CTAB (5 mM), SDS (20 mM), and TX 100 (2.5 mM). The Q-bands are magnified three times and all the spectra are shifted upward gradually for clarity.

aggregates, which takes place upon removal of the solvent. The absence of such aggregates at pH 7 supports our earlier contention regarding the higher hydrophobicity at pH 3 than at pH 7. The Soret and the Q-bands exhibit a gradual red shift from 398 to 406 nm and from 658 to 668 nm respectively on increasing the concentration of CTAB from 0 to 0.02 mM at pH 7. At pH 5, the Soret peak undergoes a red shift from 402 to 406 nm whereas a blue shift from 676 to 668 nm is observed for the Q-band upon addition of CTAB (Figure 2 b). At this pH, aggregation of chlorin p_6 has already set in and so the Q-band is red shifted compared to the solution at pH 7, in the absence of CTAB.[15] The fact that the Soret bands shift to positions identical with those at pH 7 upon addition of CTAB indicates a disruption of the pH-induced aggregates as observed for other porphyrin molecules in earlier reports.[3,9,16] With the addition of CTAB, the Soret peak undergoes only a small change at pH 3, but the absorbance increases markedly, due to the disruption of the pH-induced aggregates. A considerable shift for the Q-band from 678 to 670 nm is observed. With SDS, no change in the position of the Soret peak is observed at pH 7 as well as pH 3. For the Q-band, a small red shift from 658 to 662 nm is obtained at pH 7. However, at pH 5 and 3, blue shifts of 6 and 32 nm are observed, respectively. The considerably large shift in absorption at pH 3 indicates the formation of electrostatic SDS−chlorin p_6 cation aggregates at this pH (Figure 2). With the addition of TX-100, the Soret band undergoes a red shift of 6 and 4 nm at pH 7 and 5, respectively, whereas hardly any peak shift is observed for pH 7. The Q-band is observed to undergo a red shift of 6 nm at pH 7, but at pH 5 and 3, it experience blue shifts of 10 and 14 nm, respectively, once again due to disruption of the pH-induced aggregates by TX-100 (Figure 2d). These results are qualitatively similar to the earlier reports.[3,4,8−12,16−17,26]

Steady-State Fluorescence. On addition of CTAB to chlorin p_6 at pH 7, 5, and 3, the ϕ_f is found to pass through a minimum before increasing to a maximum value. The minimum in ϕ_f occurs at a concentration of 0.02−0.04 mM CTAB and saturation is obtained below 0.1 mM (Figures 3 and 4). This indicates a lower polarity being experienced by the fluorophore.

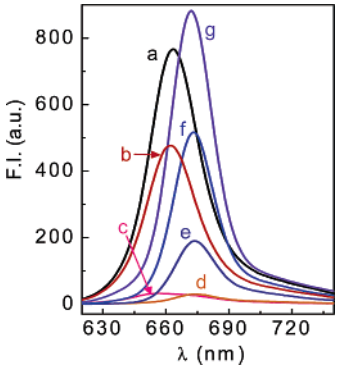

Figure 3. Fluorescence spectra of chlorin p_6 at different concentrations of CTAB at pH 7. The concentrations of CTAB used are (a) 0, (b) 0.008, (c) 0.028, (d) 0.036, (e) 0.104, (f) 0.3, and (g) 5 mM, denoted by black, red, pink, orange, royal, blue, and violet lines, respectively $\lambda_{ex} = 400$ nm.

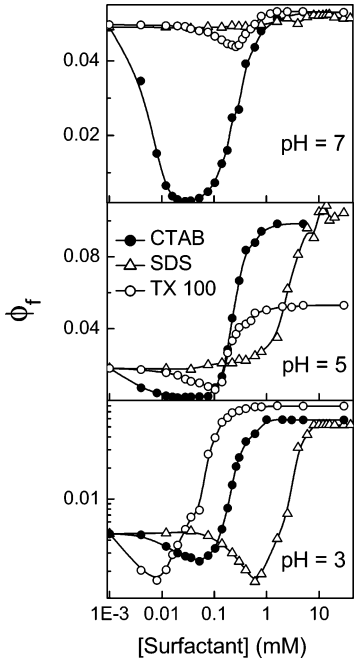

Figure 4. Variation of fluorescence quantum yields with concentration of surfactants at pH 7, 5 and 3. At pH 3, the dip is so small that it shows up only in the logarithmic scale.

Similar variations with smaller dips in ϕ_f are obtained with TX-100 and the ϕ_f^{min} and ϕ_f^{max} occur at a surfactant concentration of ca. 0.2−0.4 and 0.5 mM TX100, respectively (Figure 4). With SDS, there is no notable change in ϕ_f at pH 7, a sigmoidal increase with the point of inflection at 12 mM SDS at pH 5 and an initial dip at [SDS] = 0.6 mM followed by an increase in ϕ_f at pH 3 are observed (Figure 4). The dips appear to decrease in magnitude with a decrease in pH, as the ϕ_f also decreases with pH. The point to note is that the dip in ϕ_f with TX-100 is small at pH 7, larger at pH 5, and almost comparable to that of CTAB at pH 3, while the dip with SDS at pH 3 is more than that with other surfactants (Figure 4). The emission maximum gets shifted to 675 nm in all cases, except with SDS at pH 7, where the value is 670 nm. The shift that takes place at surfactant concentrations higher than the one required to obtain ϕ_f minimum is obtained for all the cases (Figure 4).

Time-Resolved Emission. The steady-state data can be explained in the light of aggregation and deaggregation of chlorin p_6 with surfactants, but before we do so, the time-resolved fluorescence should be discussed in order to get further

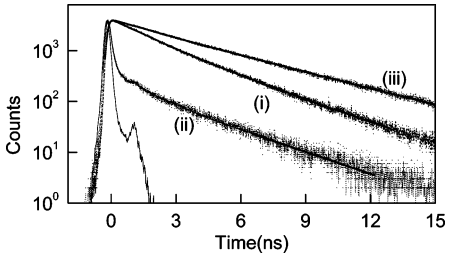

Figure 5. Fluorescence decays of chlorin p_6 at pH 5 at CTAB concentrations of (i) 0, (ii) 0.076, and (iii) 5 mM. The data are shown as dots whereas the solid lines represent the fitting curves to multiexponential functions. The instrument response function is shown along with the decays.

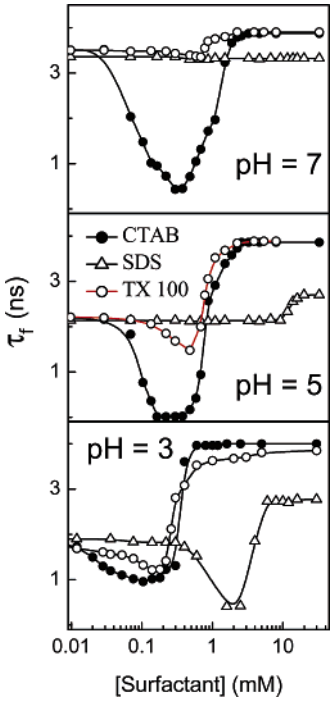

Figure 6. Variation of average lifetime as a function of concentration of surfactants at pH 7, 5, and 3.

insight of the situation. The average lifetimes (τ_f) for chlorin p_6 in the absence of surfactant are 3.5, 2.2, and 1.9 ns for pH 7, 5, and 3, respectively. At all the pH values, the lifetime initially decreases to a minimum at a concentration of CTAB of 0.052 mM (Figures 5 and 6). Similar variations of τ_f are also obtained for TX 100 for all three pH values with the minimum between 0.16 and 0.19 mM of TX100 (Figure 6). The decrease in τ_f is more prominent at pH 5, much like that in ϕ_f. Beyond the minimum point, the τ_f values increase to saturation before CMC. Such variation in radiative lifetime has been reported in earlier studies on surfactant−porphyrin complexes and is explained by the formation of fluorophore−surfactant aggregates at low surfactant concentrations, causing a decrease in ϕ_f and τ_f and subsequent solubilization in micelles.[26,31−33] Usually, such aggregation is caused by hydrophobic and electrostatic effects which reinforce each other. However, the aggregation with TX-100 indicates that such aggregation can occur due to hydrophobic effects alone, even without the assistance of electrostatic attraction, provided the fluorophore is sufficiently hydrophobic. The fact that the radiative lifetime reaches its saturation value before CMC indicates that the aggregates are disrupted completely even before micelles are formed.

On addition of SDS to solutions of chlorin p_6 at pH 7, there is a small decrease in lifetime around the CMC. This, along with the small change in ϕ_f and red shift in emission spectrum, signifies the micellar incorporation, even though there is no aggregation at low surfactant concentration, as is expected, due to the like charges of chlorin p_6 and SDS. This gains support from our earlier work, where the interaction of chlorin p_6 with methyl viologen has been shown to be modified considerably in the presence of SDS micelles, which is possible only if micellar incorporation takes place.[28] However, for pH 5, there is a significant increase in ϕ_f and τ_f with addition of SDS (Figure 6). This is because at pH 5, chlorin p_6 exists in a partially aggregated state. The addition of the surfactants leads to disruption of the pH-induced aggregates and causes an increase in the number of fluorescent monomers of the molecule. The increase in ϕ_f and τ_f is caused by this increase in the number of monomers and not by an alteration in the radiative rate. As has been indicated in our earlier studies, the overall charges of chlorin p_6 change from a negative to a positive value at pH 3, and it can be expected to form electrostatic complexes with the negatively charged SDS surfactant at low concentrations at this pH. This contention gains supports from the fact that there is no initial dip for ϕ_f and τ_f with addition of CTAB at this pH, unlike at pH 7 and 5. The steady-state and time-resolved fluorescence data substantiate this prediction as an initial decrease in the lifetime is observed followed by an increase and ultimately saturation due to incorporation in micelles. The lifetimes at maximum [SDS] at any pH have similar values, of ca. 2.7 ns. This is also true for the maximum concentration of CTAB and TX 100 systems. The lifetimes are close to 3.7 ns for all pH values. These results again reaffirm that irrespective of the pH, at micellar concentrations, the chromophore is incorporated within micelles because of favorable hydrophobic interactions.

Qualitatively, the variation of lifetimes with the concentration of surfactants (Figure 6) is similar to that of ϕ_f (Figure 4). In the case of both SDS and CTAB, the concentration at which the minimum occurs in the above plots is higher than the concentration at which the plot of quantum yield vs concentration of surfactants shows a minimum. This indicates that the quenching of fluorescence in the aggregates formed initially involves a static as well as a dynamic mechanism. At concentrations where the dissociation sets in, static quenching is hindered fast, which is marked by the increase of fluorescence intensity, However, dynamic quenching remains operative until a higher concentration of the surfactant, and so the τ starts increasing only at higher concentration, when the excess of surfactants tears away the chlorin p_6 molecules to a considerable distance from one another until finally they are sufficiently far apart so that there is no quenching at all. But in the case of TX 100, the concentrations at which minimum ϕ_f and τ_f occur are the same. This clearly indicates the absence of any electrostatic complexes between TX 100 and chlorin p_6 and the quenching in fluorescence at low TX 100 concentration is thus purely dynamic in nature. The second point to note is that at pH 5 and 3, the addition of SDS causes a 7- to 8-fold increase in the fluorescence quantum yield. However, the corresponding increase in τ_f is only by a factor of 1.2−1.5. Similarly, the addition of TX 100 at pH 5 and 3 causes a 1.7- to 2.3-fold increase in τ_f whereas the ϕ_f increases by 3- and 9-fold, respectively. This can be explained by the disruption of pH-induced aggregates by surfactants. The corresponding increase in number of fluorophores is reflected in the increase in ϕ_f. However, as the

TABLE 1: CMC, Aggregation Number of Surfactant (n), the Micelle to Fluorophore Stoichiometry (N), and the Association Constant (K_b)

surfactant	pH	n	N	10^3K_b (M^{-1})
CTAB	7.0			47 ± 4
	5.0	170	1.0	19 ± 3
	3.0			0.7 ± 0.1
	7.0			0.38 ± 0.03
SDS	5.0	62	1.0	0.90 ± 0.04
	3.0			13.6 ± 0.1

principal mechanism of quenching in pH-induced aggregates is static in nature,[15] the increase in lifetime is markedly lesser.

The association constants (K_b) obtained from the fits of the optical absorption spectra of chlorin p_6 as a function of surfactant concentration at different pH values according to eq 1 have been listed in Table 1. It is clear that K_b for CTAB at pH 7 is ~70-fold larger than that at pH 3 and the pH 5 value lies in between. This can be rationalized by a consideration of an electrostatic attraction between the dye and CTAB, which is maximum at pH 7, where the charge on the dye is almost negative. This charge decreases gradually in magnitude with a decrease in pH. However, for SDS, the K_b is higher at pH 3 and less at pH 7, which may be explained by a similar consideration that the charge on chlorin p_6 has a maximum positive value at pH 3. The results are in good agreement with the reports by Tabak and co-workers, where the binding constant for anionic TPPS4 at pH 7.5 is larger with cationic surfactant cetyl trimethylammonium chloride (CTAC) in comparison to that with zwitter ionic surfactant *N*-hexadecyl-*N*,*N*-dimethyl-3-ammonio-1-propanesulfonate (HPS). K_b is negligible for the anionic surfactant whereas it is the other way around at pH 3.0.[16]

Resonance Light-Scattering (RLS) Monitoring of Aggregation. The fluorescence results indicate the formation and disruption of aggregates as described above, but the technique is somewhat indirect in nature. To monitor the formation of aggregates by a more direct method, we have performed the resonance light-scattering (RLS) experiment. In general, in the spectral range where a solution has optical absorption, an increase in scattered light intensity can be observed as a result of the increase of the refractive index of the scattering medium in this range (RLS effect).[32] Usually this increase is masked by absorption; however, when aggregates are formed, this effect can be strong enough since the RLS intensity is proportional to the square of the scattering particle volume. Thus RLS has become an important tool for the test of formation of aggregates.[31−34]

The representative RLS spectra with CTAB and TX 100 at different pH values are shown in Figure 7. It is observed that in the absence of surfactants, the RLS spectrum of chlorin p_6 is comprised of a small trough at 400 nm, coincident with the Soret absorption. At pH 5 and 3, this trough is not perceivable. Rather, a peak is observed at 435 nm at Ph 5. Two peaks at 435 and 400 nm are observed at pH 3, indicating the presence of aggregates at these pH values. On addition of CTAB, the trough becomes shallower and a peak is formed at 435 nm for pH 7. The peak decreases beyond a surfactant concentration of 0.08 mM, which is a little more than the concentration where the minimum of ϕ_f is obtained. A similar trend is obtained with TX 100, where the peak is smaller than in CTAB, indicating a lesser degree of aggregation. In this case, maximum aggregation is obtained at a concentration of 0.05 mM. There is no change in the RLS spectra with SDS (data not shown). At pH 5 as well as pH 3, the peaks develop with the surfactants at low concentrations, indicating surfactant-induced aggregation, even

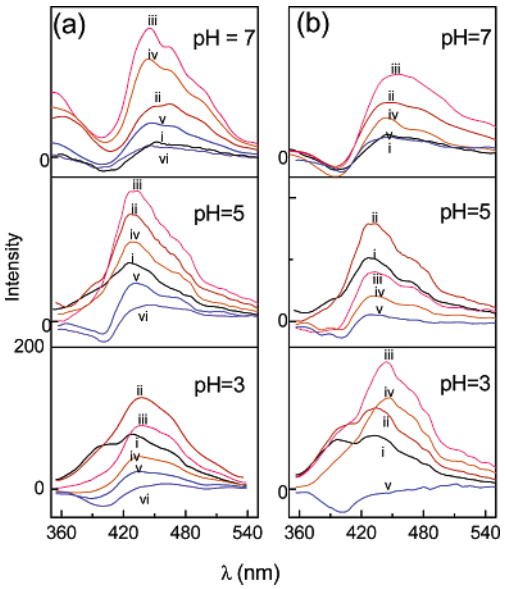

Figure 7. RLS spectrum of chlorin p_6 with (a) CTAB and (b) TX 100 at different pH values. For CTAB the concentrations are 0 (black, i), 0.05 (red, ii), 0.08 (pink, iii), 0.14 (orange, iv), 0.22 (blue, v), and 2.5 (violet, vi) mM. For TX-100, the concentrations are 0 (black, i), 0.012 (red, ii), 0.052 (pink, iii), 0.14 (orange, iv), and 2.5 (blue, v) mM.

when pH-induced aggregates are present. The increases in RLS intensities, however, are smaller than those at pH 7. The disappearance of the peak at 400 nm and increase in the intensity at 435 nm indicate a disruption of pH-induced aggregates and formation of surfactant-induced ones. The decrease in the peak and emergence of the trough at 400 nm with all three surfactants indicate a complete dissociation of the aggregates at high surfactant concentrations at all pH values. The scattering in the RLS spectra are not very large. This could be due to two reasons, small aggregation size and weak electrostatic coupling. The size of the aggregates as measured from the DLS as well as the TEM and SEM results is comparable to those obtained earlier.[35] So, we conclude that the weak electrostatic coupling in the aggregates is rather weak. This, coupled with the observation that the RLS spectra are much broader than those obtained in cases where ordered J or H aggregates have been reported, indicates that the surfactant−chlorin p_6 aggregates lack long-range order to any considerably extent. In other words, these aggregates can be classified as random aggregates. This inference is supported by the lack of sharp peaks in the absorption spectra. The RLS data for SDS at the different pH values follow the trends obtained in the absorption and fluorescence studies and do not show any evidence for ordered aggregates either.

The information about the size of the aggregates obtained from TEM and SEM micrographs is further confirmed by DLS analysis. The hydrodynamic diameter of the pH-induced aggregates measured by DLS at pH 3 is found to be 625 nm (Table 2). With an increase in CTAB concentration, the size starts increasing for low CTAB concentrations, and for 0.04 mM of CTAB, we observed aggregates with diameters of 649 nm, indicating the replacement of pH-induced aggregates by surfactant-induced aggregates. The involvement of the surfactant-induced aggregates at low CTAB concentrations is also reflected in ϕ_f, τ_f, and RLS studies, where a decrease from the initial values is obtained for the former two and an increase in the intensity is observed for the latter study. For the higher surfactant concentration, the size starts decreasing until the CMC is reached, where we observed only 12 nm particles, which is the size of CTAB micelles.[36] Disruption of the pH-induced ag-

TABLE 2: Variation of Hydrodynamic Diameter (R_h) and Polydispersity Indices (PDI) with Surfactant Concentration

	pH 3		pH 5	
[CTAB]	PDI	R_h (nm)	PDI	R_h (nm)
0	0.721 ± 0.032	625 ± 18	0.568 ± 0.021	365 ± 12
0.04	0.698 ± 0.026	649 ± 21	0.582 ± 0.024	428 ± 6
0.08	0.622 ± 0.023	256 ± 13	0.597 ± 0.019	264 ± 8
0.10	0.647 ± 0.025	113 ± 9	0.621 ± 0.023	143 ± 7
0.40	0.616 ± 0.019	89 ± 6	0.633 ± 0.024	30 ± 5
1.00	0.581 ± 0.014	31 ± 4	0.616 ± 0.017	21 ± 4
5.00	0.603 ± 0.018	12 ± 3	0.609 ± 0.019	12 ± 3

gregates and incorporation into the micelles are also reflected in the decrease in polydispersity of the solution with the addition of the surfactant. At pH 5, the diameter of the particles found from DLS in the absence of surfactant is 365 nm. From TEM, it is found to vary from 280 to 390 nm, and the density of the aggregates is much less as compared to that at pH 3. Until a concentration of 0.04 mM CTAB, the size of the particles becomes larger than that of the parent aggregates, but for the further increase in CTAB, it starts decreasing until only the micelles are observed at the CMC, which is also reflected in fluorescence and RLS measurements. This indicates the disruption of aggregates formed at lower surfactant concentrations due to incorporation in micelles.

Conclusion

Surfactants with ionic as well as nonionic headgroups are found to be capable of inducing aggregation of chlorin p_6 at submicellar concentrations. These aggregates get solubilized in micelles beyond the CMC. The aggregation with ionic surfactants can be controlled by tuning the charge on chlorin p_6, through a change in pH, as the ionic porphyrins undergo aggregation with ionic surfactants only when there is an electrostatic attraction between the headgroups and the charged fluorophore. The fact that the neutral surfactant can also induce aggregation indicates that hydrophobic effects may be sufficient for this process unless there is a hindrance due to electrostatic factors. The fluorescence of chlorin p_6 is found to be quenched statically as well as dynamically in these aggregates, unlike in pH-induced aggregates reported earlier, where the quenching is predominantly static in nature. Since the aggregates dissociate at high surfactant concentrations at all pH values, it can be concluded that the hydrophobic interaction between surfactants and chlorine p_6 is sufficient to overcome the hydrophobic interaction between the chlorine p_6 molecules, which causes them to aggregate in the first place.

Acknowledgment. This work is supported by CSIR grant no. 01(1851)/03/EMR-II.

References and Notes

(1) Service, R. F.; Szuromi, P.; Uppenbrink, J. *Science* **2002**, *295*, 2395.
(2) Whitesides, G. M.; Mathias, J. P.; Seto, C. T. *Science* **1991**, *254*, 1312.
(3) Maiti, N. C.; Mazumdar, S., Periasamy, N. *J. Phys. Chem. B* **1998**, *102*, 1528.
(4) Choi, M. Y.; Pollard, J. A.; Webb, M. A. *J. Am. Chem. Soc*. **2003**, *125*, 81.
(5) Wright, J. D. *Molecular Crystals*; Cambridge University Press: Cambridge, 1995.
(6) Brune, A.; Jeong, G.; Liddell, P. A.; Sotomura, T.; Moore, T. A.; Moore, A. L.; Gust, D. *Langmuir* 2004, *20*, 8366.
(7) Borisov, S. M.; Vasil'ev, V. V. *J. Anal. Chem.* **2004**, *59*, 155.
(8) Koti, A. S. R.; Taneja J.; Periasamy, N. *Chem. Phys. Lett.* **2003**, *375*, 17.
(9) Simlicio, F. I.; Soares, R. R.; Maionchi, F.; Santin Filho, O.; Hioka, N. *J. Phys. Chem. A* **2004**, *108*, 9384.
(10) Maiti, N. C.; Ravikanth, M.; Mazumdar S.; Periasamy, N. *J. Phys. Chem*. **1995**, 99, 17192.
(11) Kano, H.; Saito, T.; Kobayashi, T. *J. Phys. Chem. A* **2002**, 106, 3445.
(12) Kano, H.; Saito, T.; Kobayashi, T. *J. Phys. Chem. B* **2001**, 105, 413.
(13) Ricchelli, F.; Gobbo, S. *J. Photochem. Photobiol. B* **1995**, *29*, 65.
(14) Zhang, Y.-H.; Guo, L.; Ma, C.; Li, Q.-S. *Phys. Chem. Chem. Phys.* **2001**, *3*, 583.
(15) Datta, A.; Dube, A.; Jain, B.; Tiwari, A.; Gupta, P. K. *Photochem. Photobiol.* **2002**, *75*, 488.
(16) Gandini S. C. M.; Yushmanov, V. E.; Borissevitch I. E.; Tabak, M. *Langmuir* **1999**, *15*, 6233.
(17) Vermanthen, M.; Louie, E. A.; Chodosh, A. B.; Reid, S.; Simonis, U. *Langmuir* **2000**, *16*, 210.
(18) Imahori, H. *J. Phys. Chem. B* **2004**, *108*, 6130.
(19) Sharma, M.; Dube, A.; Bansal, H.; Gupta, P. K. *Photochem. Photobiol. Sci.* **2004**, *3*, 231.
(20) Das, K.; Jain, B.; Dube, A.; Gupta P. K. *Chem. Phys. Lett*. **2005**, *401*, 185.
(21) Abata, K.; Fukushima, K.; Oda, K.; Okura, I. *J. Porphyrines Phthalocyanines* **2000**, *4*, 278.
(22) *Photodynamic Therapy*; Henderson, B. W., Dougherty, T. J., Eds.; Marcel Dekker Inc.: New York, 1992.
(23) Ricchelli, F.; Gobbo, S.; Jori, G.; Vinzens, F.; Salet, C. *Photochem. Photobiol*. **1993**, *58*, 53.
(24) Nishide, H.; Tsukahara, Y.; Tsuchida, E. *J. Phys. Chem. B* **1998**, *102*, 8766.
(25) Keating, L. R.; Szalai, V. A. *Biochemistry* **2004**, *43*, 15891.
(26) Borissevitch, I. E.; Tominaga, T. T.; Imasato, H.; Tabak, M. *Anal. Chim. Acta* **1997**, *343*, 281.
(27) Mishra, P. P.; Bhatnagar, J.; Datta, A. *Chem. Phys. Lett*. **2004**, *386*, 158.
(28) Mukherjee, T. K.; Mishra, P. P.; Datta, A. *Chem. Phys. Lett.* **2005**, *407*, 119.
(29) Hoober, J. K.; Sery, T. W.; Yamamoto, N. *Photochem. Photobiol*. **1998**, *48*, 579.
(30) Seybold, P. G.; Gouterman, M. *J. Mol. Spectrosc.* **1969**, *31*, 1.
(31) Pasternack, R. F.; Collings, P. J. *Science* **1995**, *269*, 935.
(32) Pasternack, R. F.; Bustamante, C.; Collings, P. J.; Gibbs, E. J. *J. Am Chem. Soc.* **1993**, *115*, 5393.
(33) Collings, P. J.; Gibbs, E. J.; Starr, T. E.; Vafek, O.; Yee, C.; Pomerance, L. A.; Pasternack, R. F. *J. Phys. Chem. B* **1999**, *103*, 8474.
(34) Pasternack, R. F.; Fleming, C.; Herring, S.; Collings, P. J.; dePaula, J.; DeCastro, G.; Gibbs, E. J. *Biophys. J.* **2000**, *79*, 550.
(35) Koti, A. S. R.; Periasamy, N. *J. Mater. Chem.* **2002**, *12*, 2312.
(36) Berr, S. S.; Caponetti, E.; Johnson, J. S.; Jones, R. R. M.; Magid, L. J. *J. Phys. Chem.* **1986**, *90*, 5766.